Composites Science and Technology 100 (2014) 44–52

Contents lists available at ScienceDirect

Composites Science and Technology

journal homepage: www.elsevier.com/locate/compscitech

Conductive nanocomposite materials derived from SEBS-g-PPy and surface modified clay

Manzar Zahra [a], Sonia Zulfiqar [b,*], Cafer T. Yavuz [c], Hee-Seok Kweon [d], Muhammad Ilyas Sarwar [a,*]

[a] Department of Chemistry, Quaid-i-Azam University, Islamabad 45320, Pakistan
[b] Department of Chemistry, School of Natural Sciences (SNS), National University of Sciences and Technology (NUST), Islamabad 44000, Pakistan
[c] Graduate School of EEWS, Korea Advanced Institute of Science and Technology, 335 Gwahangno, Yuseong-gu, Daejeon 305-701, Republic of Korea
[d] Division of Electron Microscopic Research, Korea Basic Science Institute, 169-148 Gwahak-ro, Yuseong-gu, Daejeon 305-806, Republic of Korea

ARTICLE INFO

Article history:
Received 9 December 2013
Received in revised form 19 May 2014
Accepted 21 May 2014
Available online 2 June 2014

Keywords:
A. Nanocomposites
B. Electrical properties
B. Mechanical properties
D. Thermogravimetric analysis (TGA)
D. Transmission electron microscopy (TEM)

ABSTRACT

Conductive nanocomposites were synthesized from surface modified clay and polypyrrole grafted triblock copolymer, polystyrene-b-poly(ethylene-co-butylene)-b-polystyrene (SEBS-g-PPy). The grafting of PPy was carried out on SEBS using $FeCl_3$ as an oxidant and the formation of subsequent materials was monitored by IR, ^1H NMR spectroscopy and Gel permeation chromatography (GPC). Surface treatment of the clay was carried out by ion exchange method using the cationic salt of 2,2-bis[4-(4-aminophenoxy)phenyl]propane for better adhesion with the polymer matrix. Thin composite films containing 1–8-wt.% organoclay were investigated by FTIR, XRD, TEM, tensile testing, TGA, DSC and electrical conductivity measurements. The molar mass as determined by GPC was around 37,000. XRD pattern and TEM images described good dispersion of clay platelets in the nanocomposites. Tensile testing revealed improvement in mechanical properties up to 3-wt.% of organoclay. The bulk electrical conductivity was increased up to 7-wt.% with increase in resonance of delocalized electrons of stretched PPy chains due to hydrogen bonding with organoclay in the nanocomposites. Thermal decomposition temperatures of the nanocomposites were in the range 435–448 °C. The decomposition of the nanocomposites was observed at higher temperatures relative to the pure polymer matrix with increasing clay loading. The weight retained after 900 °C was approximately equal to the amount of organoclay added in the composites. These composite materials exhibited improvement in glass transition temperature as compared to SEBS-g-PPy.

1. Introduction

Clays have been recognized as important nano-fillers for different polymers leading to nanocomposites, which have many applications in high-tech industries including automotive, beverages and packaging [1–3]. Clay particles are often introduced into the polymer matrices to improve the toughness and strength [4–10], to increase the thermal properties [4–7], to augment barrier resistance [11–14], and to enhance the conductivity of the materials obtained. These properties are highly dependent on dispersion of nanoclays in the matrix. Among the conductive materials, clay nanocomposites have received an immense attention owing to their improved mechanical profile in combination with their conductive nature. Electrically conductive polymers such as polypyrrole, polythiophene and polyaniline have been the subject of considerable interest due to their outstanding and useful electronic, optical and redox properties [15–17]. Polypyrrole extensively studied due to its high conductivity along with good thermal and environmental stability [18] and is widely applicable in batteries, sensors, super-capacitors; microwave shielding and corrosion protection [19]. Clay/polypyrrole nanocomposites have been used as potential fillers for the insulating polymer matrices with enhanced mechanical properties and created a conductive path in the exfoliated nanocomposites lowering the conductivity value to some extent relative to intrinsic polypyrrole conductivity. Pre-synthesized polypyrrole powder as well as in situ polymerization of pyrrole monomer in thermoplastic matrix has been studied via mechanical mixing or utilizing catalysts [20]. The electrical conductivity of the nanocomposite compressed pellets sharply increased with polypyrrole loading until it leveled off to the value of bulk powder polypyrrole. However, its less solubility limits the processability and physical properties of the materials in practical

* Corresponding authors. Tel.: +92 301 5017753; fax: +92 51 90855552 (S. Zulfiqar). Tel.: +92 51 90642132; fax: +92 51 90642241 (M.I. Sarwar).
E-mail addresses: soniazulfiqar@yahoo.com (S. Zulfiqar), ilyassarwar@hotmail.com (M.I. Sarwar).

http://dx.doi.org/10.1016/j.compscitech.2014.05.025
0266-3538/

relevance. So, it opens up a new field of clay nanocomposite with best qualities of each component i.e., conductive and plastic properties of the polymer along with enhanced mechanical properties due to presence of clay layers [21–23]. Polypropylene-polypyrrole/clay nanocomposites have also been reported and the conductivity of the nanocomposites is dictated by the relative proportion of polypyrrole and montmorillonite [24].

Polystyrene-b-poly(ethylene-co-butylene)-b-polystyrene, a thermoplastic elastomer has been variously used due to its advantageous properties like, higher hardness, abrasion resistance, tensile strength and flexural modulus. It has been modified for formation of composites as well as hybrid materials with enhanced mechanical and thermal properties [25]. Polystyrene-b-poly (ethylene-co-butylene)-b-polystyrene-grafted-maleic anhydride (SEBS-g-MA) based hybrid materials with enhanced mechanical properties have been reported [26]. Conductive clay composites are now being produced with great interest due to controlled electrical conductivity with good thermal and mechanical stability. Polypyrrole was produced into the clay interlayer spacings via inverted emulsion polymerization using dodecylbenzenesulphonic acid (DBSA) as an emulsifier and a dopant. Temperature dependence of dc conductivity was demonstrated an increase in conductivity with temperature, while at room temperature polypyrrole dc conductivity was found to be higher i.e., 20 S/cm as compared to ~6 S/cm of nanocomposites [27].

In this attempt, polypyrrole was grafted on SEBS to make it conductive using $FeCl_3$ as an oxidant. The resulting SEBS-g-PPy was characterized by FT-IR, ^{1}H-NMR techniques. The hydrophilic nature of clay was changed to organophilic using 2,2-bis[4-(4-aminophenoxy) phenyl]propane as intercalating agent through ion exchange method. Thin nanocomposite films were produced by varying the proportion of the organoclay using solution intercalation method and then evaporating the solvent. The clay developed hydrogen bonding with the polypyrrole stretching the chains in a linear fashion to increase the resonance of delocalized electrons of polypyrrole with improved bulk electrical conductivity of the resulting nanocomposites. The characterization of the hybrid films was carried out using various techniques to investigate the morphology, mechanical, thermal and electrical properties.

2. Experimental

2.1. Materials

SEBS elastomer with 28% styrene content and having average molecular weight 118,000, supplied by Aldrich was used in the synthesis of nanocomposites. Montmorillonite (MMT) and 2,2-bis[4-(4-aminophenoxy)phenyl]propane (BAPPP) (98%) were procured from Aldrich and were used as received. Methanol (99.5%) and chloroform (99%) were purchased from Merck and the later was used after drying. Pyrrole (96%) and hydrochloric acid (99%) were purchased from Fluka while anhydrous ferric chloride (98%), dimethyl sulphoxide (DMSO) (99.5%) and acetone were provided by Reidel-de Haen. The reagent, silver nitrate was taken from BDH. Chloroform was dried by the addition of anhydrous calcium chloride and distilling at constant boiling temperature. The filtrate was refluxed and then collected at 60 °C for use in the present work.

2.2. Synthesis of SEBS-g-PPy

Triblock copolymer SEBS (5.0 g) was dissolved in chloroform (50 mL) with continuous stirring for 24 h. After the complete dissolution, polymer solution was heated to 60 °C with constant stirring, followed by the addition of anhydrous $FeCl_3$ (1.38 g) as a catalyst. A homogeneous mixture was obtained in 15 min. Pyrrole was freshly distilled under reduced pressure to remove any inhibitor present and was kept in dark at lower temperature. Then pyrrole (5.9 mL) was injected drop-wise to the above solution. The color of reaction mixture was changed to dark black immediately indicating the formation of polypyrrole and the refluxing was continued for 3 h at 60 °C. The black mass was soluble in chloroform and was separated using methanol. The resulting rubbery mass was repeatedly washed with methanol and distilled water to remove the characteristic color of ferric chloride and finally with acetone. The SEBS-g-PPy was collected and dried under vacuum for 72 h. The chemical reactions leading to the formation of SEBS-g-PPy is presented in Scheme 1. FTIR (KBr) of SEBS-g-PPy: 3295 and 1566 cm^{-1} (sec. amine N—H stretch and bend), 1180 cm^{-1} (C—N stretch), 3025 and 2958 cm^{-1} (aromatic C—H stretch), 1600 and 1492 cm^{-1} (aromatic C=C stretch), 841 cm^{-1} (*p*-disubstitution), 2918 and 2849 cm^{-1} (aliphatic C—H stretch), 1453 and 1372 cm^{-1} (aliphatic C—H bend). ^{1}H NMR (300 MHz, $CDCl_3$, δ_H ppm): 0.9–2.0 (aliphatic protons), 6.4–6.6 (pyrrole ring protons) 7.63 (proton attached to nitrogen of pyrrole), 7.0–7.3 (aromatic protons).

2.3. Intercalation of montmorillonite

To improve good adhesion between hydrophilic clay and SEBS-g-PPy matrix, MMT was organically modified with BAPPP (an intercalating agent) using ion-exchange method. For this purpose, BAPPP (12.5 g) was dissolved in DMSO (60 mL), followed by the addition of HCl (3.6 mL) and heating to 80 °C formed the quaternary ammonium cations (Scheme 2). MMT (5 g) was dispersed in DMSO (50 mL) at 80 °C in a separate beaker. This dispersion of MMT was added to the solution of ammonium salt of BAPPP and the mixture was agitated vigorously for 3 h at 80 °C. The precipitate was filtered after cooling to room temperature. The precipitate was then poured into a 500 mL beaker with 200 mL DMSO with vigorously stirring for 1 h and again filtered. This procedure was repeated until the filtrate gave no precipitate with 0.1 N $AgNO_3$ solution, thus indicating presence of no free chloride ions with the organically modified clay (OMMT). The final product was dried in vacuum oven for 24 h at 60 °C. It was finely ground before the nanocomposite formation. The intercalation of MMT is pictorially shown in Scheme 3.

2.4. Formation of nanocomposites

A stock solution of SEBS-g-PPy was prepared by dissolving 10 g copolymer in 60 g of chloroform. A known amount of stock solution was transferred in 25 mL flask and then OMMT was added in required proportions for a particular concentration with constant stirring for 24 h at room temperature. The mixture was poured into the glass petri dish and allowed to stand overnight to evaporate the solvent resulting in the formation of nanocomposite film. Various other concentrations of the composite films were prepared in the similar technique. These thin films were then dried under vacuum for 72 h at room temperature to constant weight. The formation of nanocomposite films is illustrated in Scheme 4. FTIR (KBr) of SEBS-g-PPy/OMMT nanocomposites: 3296 and 1584 cm^{-1} (sec. amine N—H stretch and bend), 3025 and 2958 cm^{-1} (aromatic C—H stretch), 1600 and 1492 cm^{-1} (aromatic C=C stretch), 2918 and 2849 cm^{-1} (aliphatic C—H stretch), 1453 and 1377 cm^{-1} (aliphatic C—H bend), 1015 cm^{-1} (Si—O—Si linkage).

2.5. Characterization techniques

The chemical structures of SEBS-g-PPy and nanocomposites were verified by FTIR in the range 4000–400 cm^{-1} using Thermo Nicolet 6700 FTIR Spectrophotometer. The grafting of copolymer

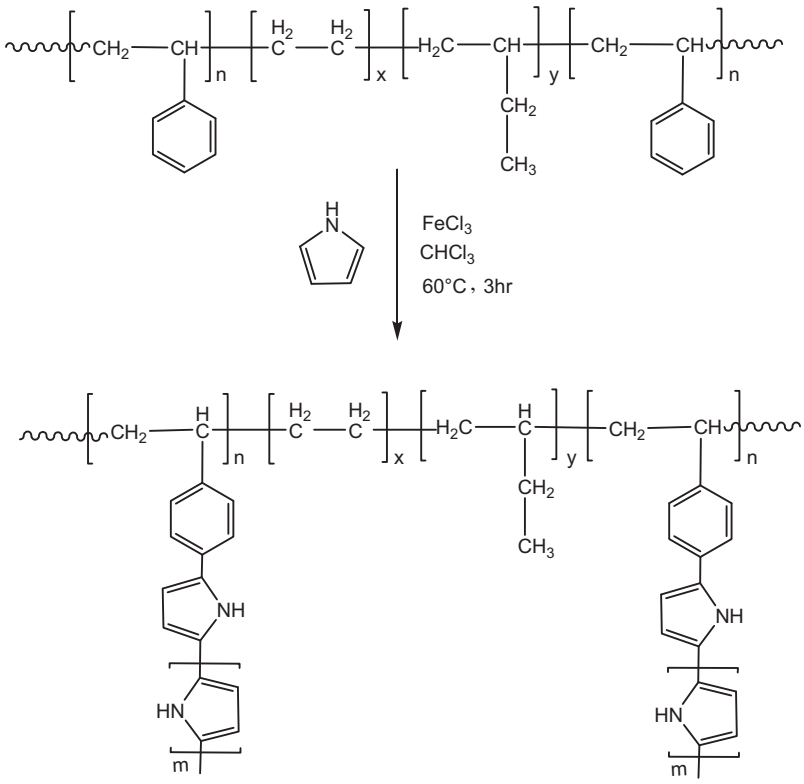

Scheme 1. Chemical reactions leading to the formation of SEBS-g-PPy.

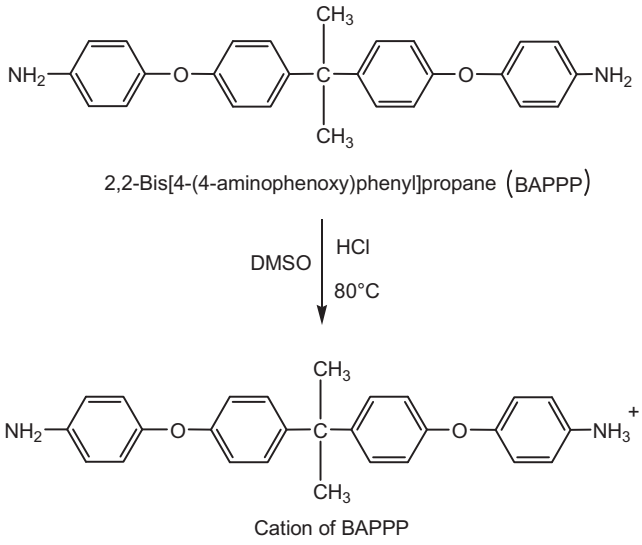

Scheme 2. The formation of quaternary ammonium cation of intercalating agent.

was further confirmed by ^{1}H NMR analysis using $CDCl_3$ as a solvent with BRUKER Spectrometer operating at 300.13 MHz. The molar mass was calculated through GPC using THF as an eluent and refractive index (RI) detector. The diffraction pattern of neat MMT, OMMT and SEBS-g-PPy/OMMT nanocomposites was studied in the reflection mode (radiation wavelength = 0.154 nm) over the range $2\theta = 2^\circ$ and 10° with a step size of 0.02° using X-ray diffractrometer 3040/60XPert PRO PAN analytical. Nanostructures of materials were monitored using FEI Tecnai G2 Spirit Twin transmission electron microscope, operated at an accelerating voltage of 120 kV. The nanocomposite films were first microtomed into 30 nm ultra thin sections with the help of diamond knife using Leica Ultracut UCT ultramicrotome. The dc electrical conductivity of the films was measured by means of the standard four probe technique. Thin films were directly subjected to 50 or 100 Voltage and the respective resistivity was recorded which then was converted to conductivity. High resistance meter with a model 6517A of Kaithly (USA) having the resistance range $1000–10^{17}\ \Omega$ has been used for the resistivity measurement of the samples. Mechanical properties of the nanocomposites (rectangular strips) with dimensions (ca. $14 \times 6.0–7.0 \times 0.10–0.25$ mm) were measured according to DIN procedure 53455 having a crosshead speed

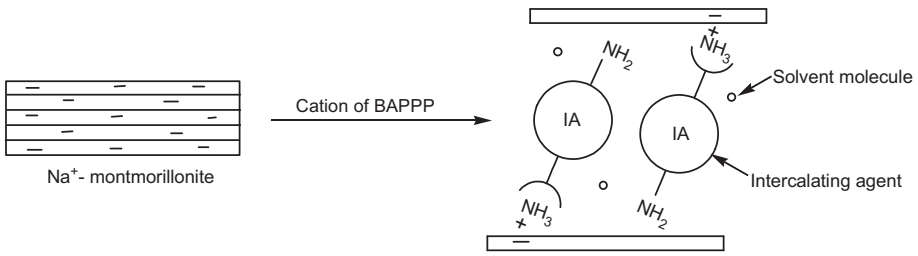

Scheme 3. The formation of OMMT through solution intercalation technique.

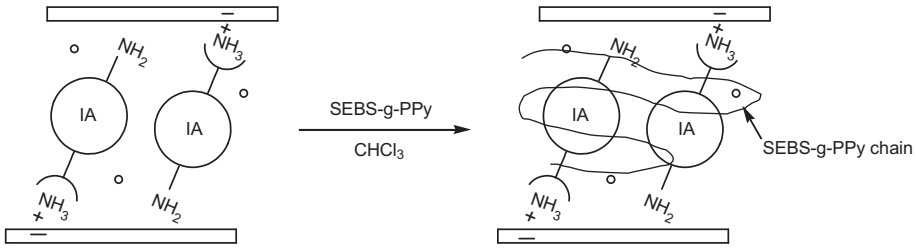

Scheme 4. Synthesis of conductive SEBS-g-PPy/OMMT nanocomposites.

of 5 mm min^{-1} at 25 °C using Testometric Universal Testing machine, M500-30CT. The pneumatic gripping system was used to avoid the slipping of the strips and an average value obtained from 4 to 5 different measurements in each case has been described. Thermal stability of the nanocomposites was determined using NETZSCH TG 209 F3 thermogravimetric analyzer using 1–5 mg of the sample in Al_2O_3 crucible heated from 25 to 900 °C at a heating rate of 10 °C/min under nitrogen atmosphere with a gas flow rate of 20 mL/min. Glass transition temperature was monitored by NETZSCH TG 209 F3 differential scanning calorimeter taking 5–10 mg of samples in aluminum pans and heated at a rate of 10 °C/min.

3. Results and discussion

The structural elucidation of SEBS-g-PPy and nanocomposites were determined by IR spectroscopy. ^{1}HNMR was also recorded for further confirmation of SEBS-g-PPy formation. Moreover, molar mass of SEBS-g-PPy revealed around 37,000. The pure SEBS has very poor film forming property and did not give smooth film. However, upon grafting of the polypyrrole on backbone of SEBS, the film forming property was improved and SEBS-g-PPy produced very smooth and well textured film. Nanocomposites films obtained from SEBS-g-PPy/OMMT were opaque and dark black in color. Different analyses carried out for the characterization of these materials are described below.

3.1. Spectroscopic analyses

The characteristic IR bands of SEBS-g-PPy including both aromatic and aliphatic CH_2 observed at their respective positions (Fig. 1) Appearance of new bands for polypyrrole verified the presence of pyrrole moiety in SEBS-g-PPy. The grafting of polypyrrole at *para* position of phenyl ring of polystyrene (PS) block appeared at 841 cm^{-1} is in good agreement with the reported value. ^{1}H NMR of SEBS-g-PPy was taken in $CDCl_3$ solvent and analyzed according to the chemical shift values for various protons experiencing different chemical environment present in the polymer chain (Fig. 2). All the characteristic protons of the polymer chain gave their signals. Signals observed in the region from 0.9 to 2.0 ppm belonged to the aliphatic protons. Pyrrole ring protons gave their signals at 6.489 and 6.598 ppm with a broad signal observed at 7.632 ppm due to the proton attached to nitrogen of pyrrole. Aromatic ring protons gave signals between 7.0 and 7.3 ppm. The IR and ^{1}H NMR data confirmed the grafting of PPy on the SEBS. A new band for SEBS-g-PPy/OMMT nanocomposites appeared at 1015 cm^{-1} due to the presence of Si—O—Si linkage of the clay. Another characteristic bending vibration of pyrrole N—H at 1566 cm^{-1} shifted to higher frequency i.e., 1584 cm^{-1}. This band shifting was due to the formation of H-bonding between PPy and clay as depicted in Fig. 3. Due to this reason the absorption of N—H bending shifted to higher wave number, as the free N—H bending of pyrrole was restricted during H-bond formation. Therefore, appearance of Si—O—Si linkage and this band shifting confirmed the formation of hybrid nanomaterials.

3.2. X-ray diffraction analysis

The level of clay dispersion in the nanocomposites was monitored by recording XRD patterns of neat MMT, OMMT and nanocomposite as shown in Fig. 4. The characteristic peak for MMT was observed at around $2\theta = 8.91°$ giving a d-spacing 0.99 nm corresponding to (001) reflection. After intercalation, this peak was shifted to the lower 2θ value i.e., 4.52° giving a more d-spacing (d = 1.95 nm). This shifting of (001) reflection toward lower 2θ suggested intercalation of MMT due to the replacement of Na^+ with large sized cationic aromatic diamine, BAPPP. Nanocomposites film containing 2-wt.% OMMT gave no characteristic peak of clay in the low 2θ angle suggesting either an immiscible system was formed or clay dispersed homogeneously in the form of individual layers within the matrix. These observations led to the formation of intercalation and partially exfoliated nanocomposites. Further increased d-spacing permitted SEBS-g-PPy chains to move into the interlayer of clay for a uniform dispersion and adhesion between the phases. However, XRD results provide incomplete information about the extent of nanolayers dispersion and some additional information is required to verify homogeneous OMMT dispersion.

3.3. Microscopic analysis

The dispersion of clay layers can be seen more clearly by viewing images of ultrathin samples under TEM as XRD pattern gave incomplete information about the level of dispersion including no peak representing delaminated clay. Therefore, the nanostructure of the hybrid materials was monitored by TEM and the micrographs are shown in Fig. 5. High resolution micrographs recorded for 2, 3 and 5-wt.% OMMT/nanocomposites disclosed dispersion of OMMT implying as a mixed intercalated/delaminated silicate layers in SEBS-g-PPy matrix. These results may in complete agreement with that of the XRD pattern with 2-wt.% OMMT indicating amorphous nature of the nanocomposites due to ample dispersion and proved the formation of the nanocomposites. At higher concentration of OMMT (7-wt.%) in hybrid materials, individual clay platelets were predominant with some tactoids indicating that the morphology was partially exfoliated and partially intercalated. However, the dimensions of these stacks are too small to give any diffraction peak in the XRD pattern. Mechanical properties were improved up to 3-wt.% of clay, so it is concluded that at lower concentrations better dispersion of clay layers was achieved in the polymer matrix, thus resulting increased tensile strength of the nanocomposites.

3.4. Conductivity of clay nanocomposites

SEBS is altogether an insulating thermoplastic elastomer, while polypyrrole is a conducting polymer with conductivity value up to

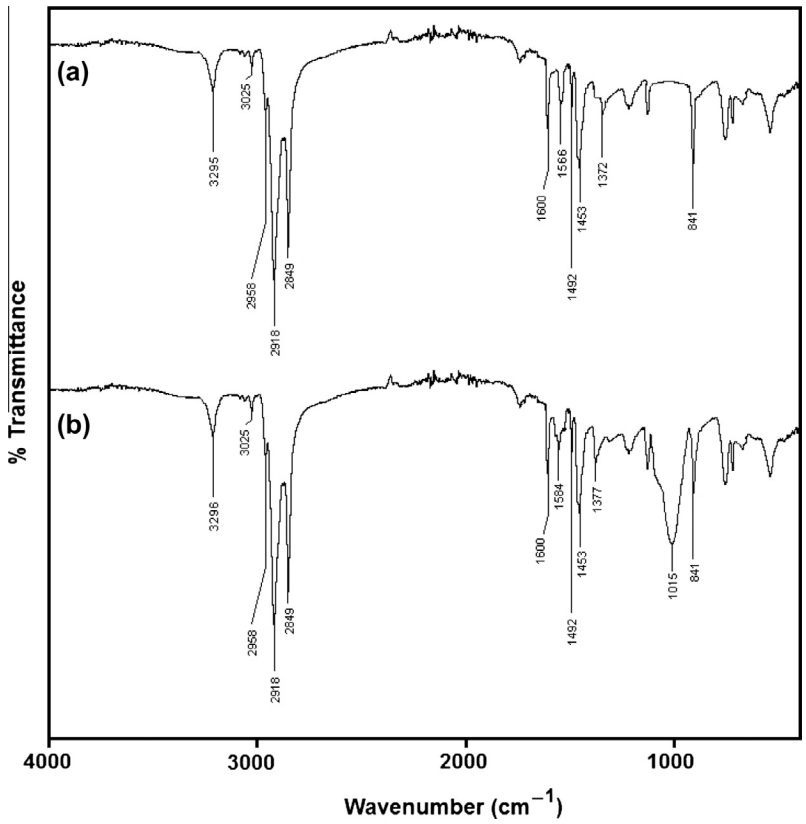

Fig. 1. FTIR Spectra of (a) SEBS-g-PPy and (b) SEBS-g-PPy/clay nanocomposite.

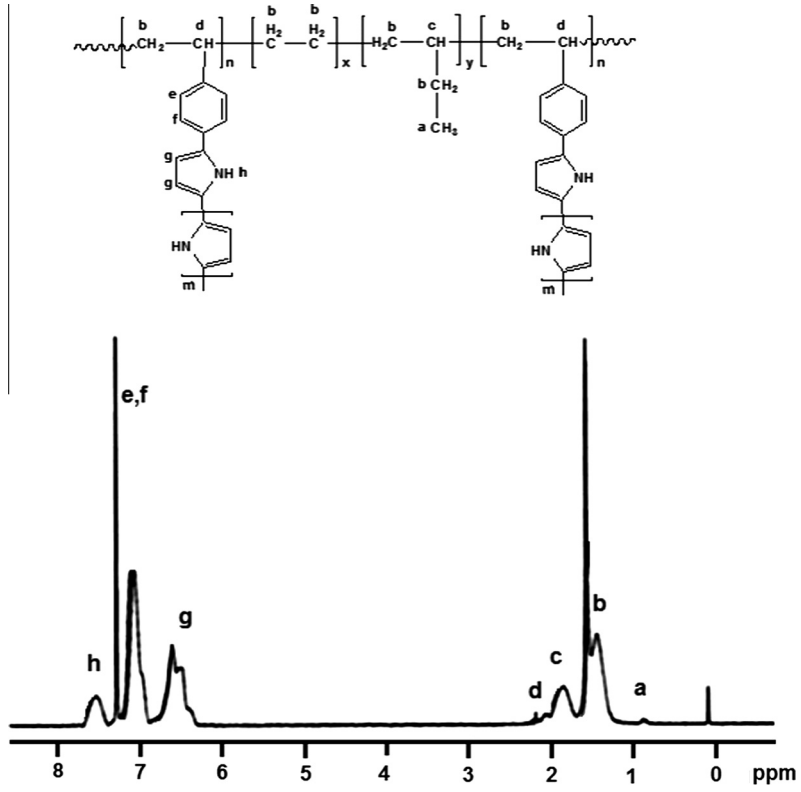

Fig. 2. ^{1}H NMR Spectrum of SEBS-g-PPy.

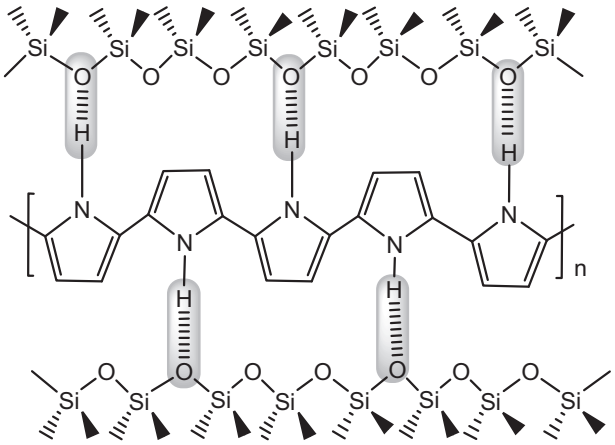

Fig. 3. H-bonding between polypyrrole and silicate group of clay.

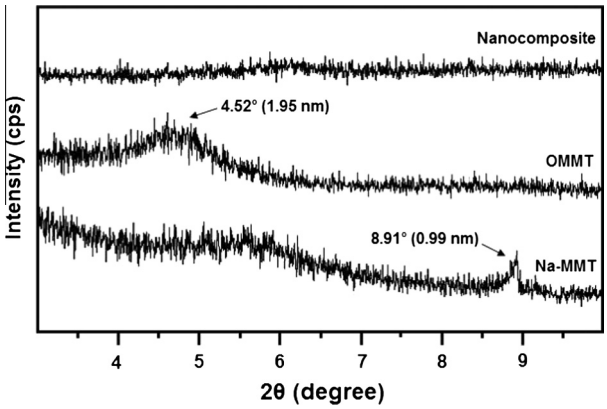

Fig. 4. XRD pattern of MMT, OMMT and SEBS-g-PPy/OMMT nanocomposite.

100 S/cm. When the later grafted on SEBS at benzene ring of styrene block improved the film-forming property of the materials and also resulted in an increase in conductivity of the insulating matrix. The value of conductivity for SEBS-g-PPy was measured to be −13.698 (Table 1). In fact, resistivity of these materials was measured using four probe method at room temperature and their corresponding conductivity values were then plotted against the clay content. Fig. 6 shows the behavior of log conductivity as function of clay content. Conductivity initially showed a gradual increase with increase in clay content but a sharp increase was detected up to 6–7-wt.% clay loading and then its value went to decline. Optimum value of log conductivity was observed with 7-wt.% of OMMT loading that is −8.496 (Table 1). Increase in conductivity, even with the insulating clay was attributed to the stretched PPy chains in the clay interlayer spacings. As these interlayer spacings are of the atomic or molecular levels, so PPy chains are supposed to be in stretched form. Due to this reason π electron delocalization may increase which facilitates the flow of electric current. One of the other reasons of this confinement of polymer chain is the formation of very strong hydrogen bonding between the polar N—H group of the polypyrrole and the silicate moieties of the clay layers which are directed out of the clay layers. On the other hand, in the pure SEBS-g-PPy sample, the polymer chains are much entangled and disordered that the delocalized electrons cannot flow easily relative to the hydrogen bonded SEBS-g-PPy/OMMT nanocomposites. After 7-wt.%, there was a decrease in conductivity because the insulating character of the clay became dominant over the conductive nature of polymer. Highly conductive core–shell nanocomposites have been produced using poly(N-vinylcarbazole) (PNVC)-polypyrrole (PPy) with MWNTs, free radical mechanism was exploited between the cation radical and nanotubes using ferric chloride as an oxidant. SEM and TEM confirmed the coating of copolymer on the surface of the nanotubes. The conductivity of the resulting nanocomposite was increased as compared to PNVC [28]. Clay/PPy nanocomposites with loadings 5, 10, 15 and 25-wt.% polypyrrole have been reported which were dark grey in color and became deep black at high loadings of PPy. The electrical conductivity of the nanocomposite compressed pellets sharply increased with polypyrrole loading until it leveled off to the value of bulk powder polypyrrole [20]. Conducting nanocomposites of polystyrene or styrene/acrylonitrile copolymer–clay have been produced with controlled conductivity, increased mechanical and thermal properties. The polypyrrole (PPy) was produced into the clay layers by inverted emulsion polymerization using dodecylbenzenesulphonic acid (DBSA) as an emulsifier and a dopant. Temperature dependence of DC conductivity was increased with temperature while at room temperature PPy DC conductivity was found to be higher i.e., 20 S/cm as compared to ∼6 S/cm of nanocomposites [27]. Polypyrrole has been prepared in the nanolayers by in situ polymerization of monomer in the presence of clay forming the clay/PPy nanocomposites [20]. TEM showed increased interlamellar spacing of untreated clay. Conductivity was increased with increase in PPy content. Polypyrrole graft copolymer/clay nanocomposites have been made by in situ polymerization of pyrrole monomer onto pre-exfoliated water soluble poly(styrenesulfonic acid-*co*-pyrrolylmethyl styrene) (P(SSA-*co*-PMS))/clay nanocomposites or by simple blending of poly(styrenesulphonic acid-*g*-pyrrole) (PSSA-*g*-PPy) with clay. These composites were characterized to be exfoliated in nature, as clay content was increased the composite conductivity was decreased [29]. However, the overall low conductivity values of SEBS-g-PPy/clay nanocomposites might be due to lesser amount of pyrrole used to retain the film-forming property. The SEBS to pyrrole ratio employed was 1:1.7 respectively. The other reason presumably caused by an insulating surface layer of SEBS on composite surface. More conductive materials can also be synthesized with increased pyrrole content in the reaction, which results PPy particles suspended in the medium that was not the reaction of choice. Conductivity with good processability and mechanical profile was the point of focus, so conductivity was to be compromised a little.

3.5. Mechanical properties

The mechanical properties of the nanocomposites were improved relative to the SEBS-g-PPy matrix. The stress–strain isotherms for various clay compositions exhibited better mechanical properties of the nanocomposites than the matrix as indicated in Fig. 7 and Table 2. The ultimate stress of the system increased upon the addition of OMMT in SEBS-g-PPy matrix. The maximum stress value for SEBS-g-PPy was 13.48 MPa which increased up to 17.98 MPa with 3-wt.% of OMMT and on further addition of clay, the value of stress decreased. Similar behavior was observed with the % elongation that increased from 267% to 284% in 3-wt.% addition of organoclay. Toughness of the composites displayed a very sharp increase when 1% organoclay was added into the polymeric system, this variation revealed improvement in toughness up to 3-wt.%, and beyond this concentration, it decreased. Tensile modulus increased sharply as compared to SEBS-g-PPy (71.3 MPa) up to 403.4 MPa with 3-wt.% clay loading but then decreased due to the increase in brittleness of nanocomposites.

Introduction of clay platelets into the organic matrix provides reinforcement up to a certain limit and then further addition of nanolayers deteriorates the properties. Organic phase cannot withstand high stresses, as it has low glass transition temperature and

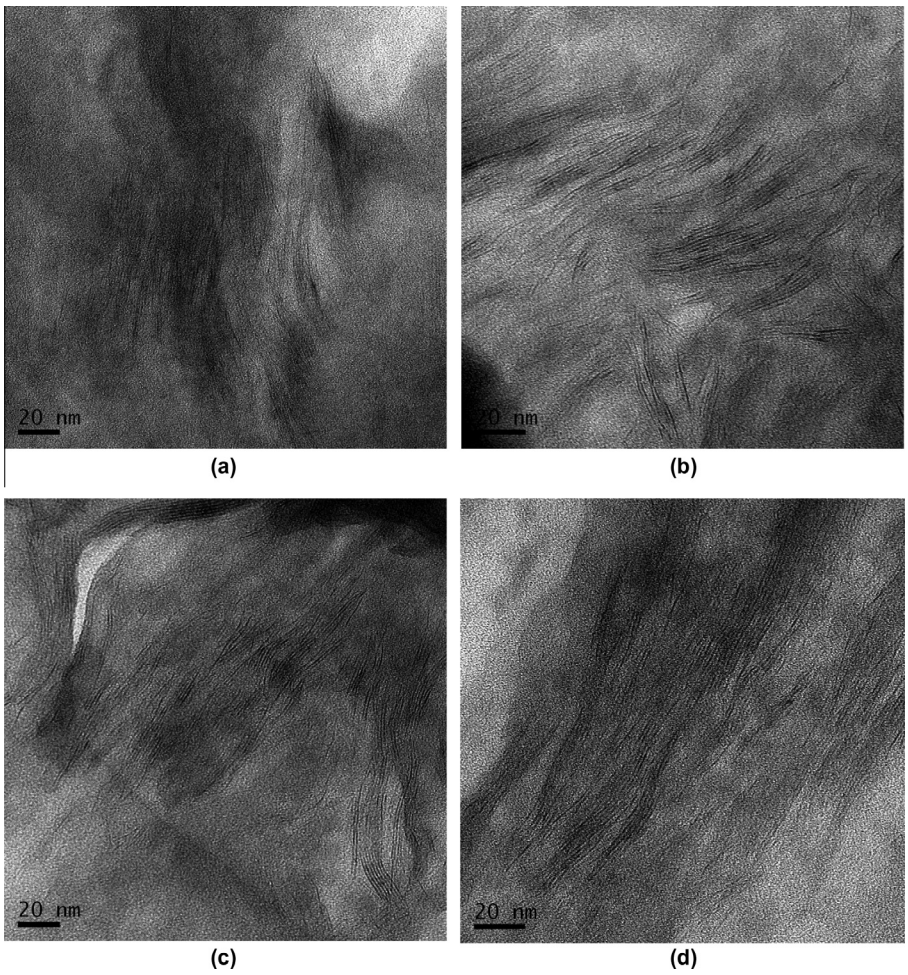

Fig. 5. TEM micrographs of SEBS-g-PPy/OMMT nanocomposites (a) 2-wt.%, (b) 3-wt.%, (c) 5-wt.% and (d) 7-wt.% clay contents.

Table 1
Log conductivity data of SEBS-g-PPy/OMMT nanocomposites.

Clay content (%)	Log conductivity (σ)
0	−13.698
1	−12.886
2	−12.824
3	−9.752
4	−9.278
5	−9.225
6	−8.907
7	−8.496
8	−9.245

large free volume but when a reinforcement having high glass transition temperature and small free volume is added into it, the resulting composites have the capability of tolerating large stresses. This intimate mixing of both the organic and inorganic phases results in overall improved properties of the nanocomposites. As the clay concentration increased beyond 3–5-wt.%, agglomeration of the silicate layers may result in aggregation of clay platelets making the distribution irregular. This increased particle size makes the material more porous, thus deteriorating the material properties at higher clay content. With the increase in the clay concentration from 3 to 5-wt.%, an increase in maximum stress, strain, toughness and modulus values to some extent was observed. This behavior may be dictated due to the addition intercalation of the clay layers in the nanocomposites.

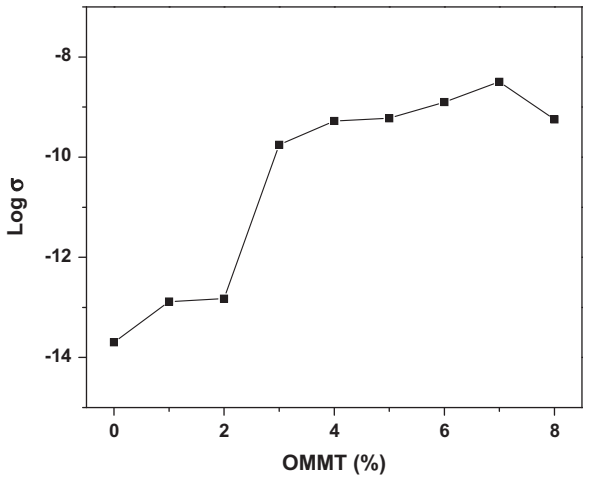

Fig. 6. Log conductivity of SEBS-g-PPy/OMMT nanocomposites vs. clay content.

3.6. Thermogravimetric analysis

Thermal stability of the nanocomposites was determined using thermogravimetric analysis (TGA) under inert atmosphere and the thermograms for this system were obtained in the temperature range 25–900 °C as shown in Fig. 8. Thermal decomposition temperatures SEBS-g-PPy and hybrid materials were in the range

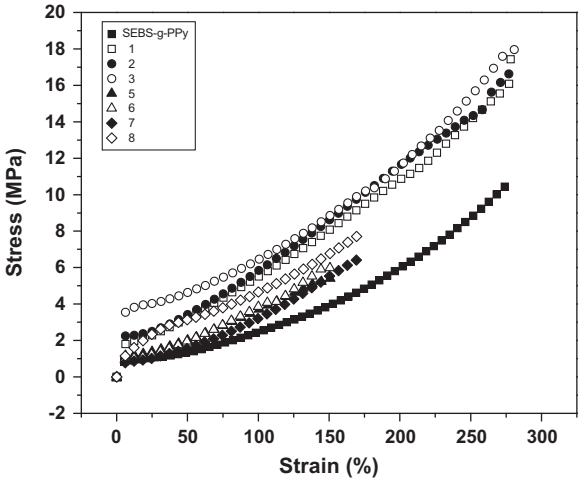

Fig. 7. Tensile behavior of SEBS-g-PPy/OMMT nanocomposites.

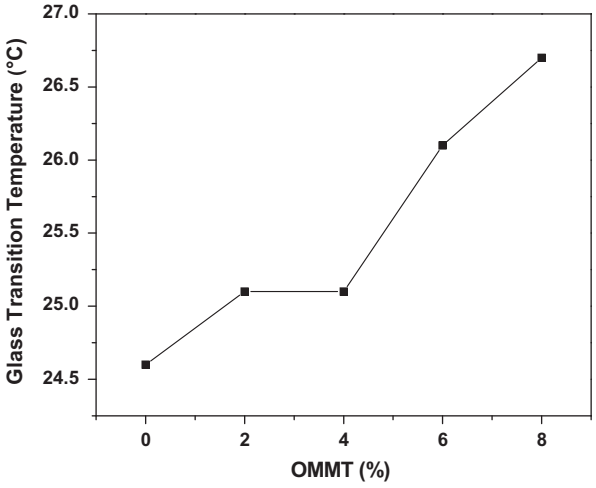

Fig. 9. Variation in glass transition temperatures of SEBS-g-PPy/OMMT nanocomposites vs. clay content.

435–448 °C and thermal stability increased with increase in OMMT loading. Increase in the thermal stability was achieved due to incorporation of inorganic phase which offered more resistance to elevated temperature making the material suitable for use at high temperature [30,31]. Nanocomposites prepared from powered PPy and OMMT decomposed in two steps that might be due to degradation of PPy. [32]. SEBS is a thermoplastic elastomer having excellent thermal stability and decomposes in single step. Similar behavior was indicated by SEBS-g-PPy and its nanocomposites with OMMT as given in Fig. 8. The weights of residues left after the decomposition at 900 °C were roughly proportional to the clay content in the nanocomposites.

Table 2
Mechanical properties of SEBS-g-PPy/OMMT nanocomposites.

Clay content (%)	Max. stress (MPa) ±1.0	Max. strain (%) ±0.02	Toughness (MPa) ±0.2	Tensile modulus (MPa) ±0.02
0	13.48	267.5	116.7	71.3
1	16.96	274.6	2193.6	250.8
2	17.67	279.0	2319.0	334.4
3	17.98	284.4	2567.4	403.4
5	7.50	186.5	1111.0	198.8
6	5.55	159.3	462.3	132.2
7	6.50	172.8	523.8	144.8
8	7.75	170.2	729.2	96.0

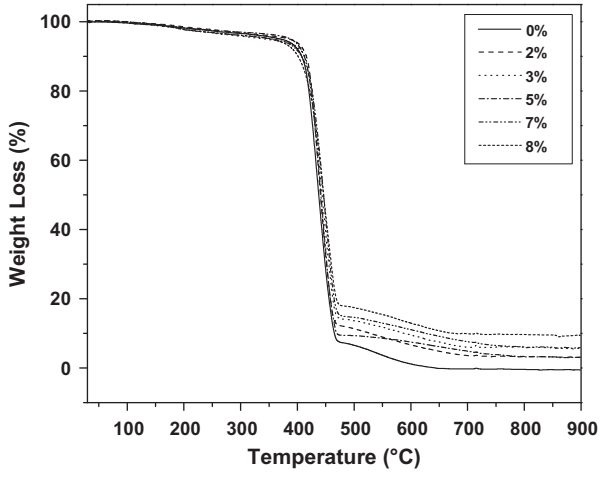

Fig. 8. TGA curves of SEBS-g-PPy/OMMT nanocomposites.

3.7. Differential scanning calorimetry

The glass transition temperatures (T_g) of SEBS-g-PPy/OMMT nanocomposites are presented in Fig. 9. The data indicated a slight increase in the T_g values with increasing clay content in the matrix. SEBS-g-PPy showed a T_g value 24.6 °C and it increased gradually with addition of OMMT. Increased amount of OMMT impeded the segmental motion of the polymer chains, thus shifting the T_g toward high temperature. This observation implied that more interactions between the two phases. Therefore, the motion of SEBS-g-PPy chains was restricted, thus slightly increasing the T_g values of nanocomposites. T_g of composites augmented relative to SEBS-g-PPy due to mutual interaction of both the phases suppressing the mobility of the polymer segments near the interface.

4. Conclusions

SEBS-g-PPy/OMMT nanocomposites were successfully prepared by solution intercalation method. The incorporation of OMMT reinforced the SEBS-g-PPy matrix depicting good compatibility between the two phases through hydrogen bonding. These interfacial interactions through hydrogen bonding promoted strong adhesion between the two disparate phases overcoming the stress transfer problem. Therefore, these interactions resulted in enhanced thermo-mechanical properties of the nanocomposites. The dispersion of individual silicate sheet was optimum at low clay concentration, giving observed increase in the mechanical properties of these materials. At high clay loading, it might exist in the form of agglomerates with lesser cohesion with organic matrix and caused adverse effects on the mechanical properties. The bulk electrical conductivity was increased up to 7-wt.%, which was due to increase in resonance of delocalized electrons of stretched PPy chains due to hydrogen bonding with organoclay in the nanocomposites. The thermal stability of hybrid materials was also increased by corresponding increase in OMMT content in the matrix.

References

[1] Giannelis EP. Adv Mater 1996;8:2935.
[2] Lagaly G, Pinnavaia TJ. Applied clay science. Amsterdam: Elsevier; 1999.

[3] Pinnavaia TJ, Beall GW. Polymer clay nanocomposites. New York: Wiley; 2001.
[4] Zulfiqar S, Sarwar MI. Nanoscale Res Lett 2009;4:391399.
[5] Zulfiqar S, Rafique M, Shaukat MS, Ishaq M, Sarwar MI. Colloid Polym Sci 2009;287:715723.
[6] Burnside SD, Giannelis EP. Chem Mater 1995;7:1597–600.
[7] Sarfaraz A, Warsi MF, Sarwar MI, Ishaq M. Bull Mater Sci 2012;35:539–44.
[8] Zulfiqar S, Ahmad Z, Sarwar MI. Aust J Chem 2009;62:441447.
[9] Zulfiqar S, Sarwar MI. Solid State Sci 2009;11:12461251.
[10] Zulfiqar S, Ahmad Z, Ishaq M, Sarwar MI. Mater Sci Eng A 2009;525:3036.
[11] Gao F. Mater Today 2004;7:5055.
[12] Yano Y, Usuki A, Kurauchi T, Kamigato O. J Polym Sci Part A Polym Chem 1993;31:24932498.
[13] Messersmith PB, Giannelis EP. Chem Mater 1994;6:1719–25.
[14] Ciardeli F, Coiai S, Passaglia E, Pucci A, Ruggeri G. Polym Int 2008;57:805–36.
[15] Skotheim TA. Hand book of conducting polymers. New York: Marcel Dekker; 1986.
[16] Dao LH, Leclerc M, Guay J, Chevalier JW. Synth Met 1989;29:377–82.
[17] Li S, Cao Y, Xue Z. Synth Met 1987;20:141–9.
[18] Joo J, Lee JK, Lee SY, Jang KS, Oh EJ, Epstein AJ. Macromolecules 2001;33:5131–6.
[19] Lu Y, Shi G, Li C, Liang Y. J Appl Polym Sci 1998;70:2169–72.
[20] Boukerma K, Piquemal JY, Chehimi MM, Mravcakova M, Omastova M, Beaunier P. Polymer 2006;47:569–76.
[21] Ruiz-Hitzky E, Aranda P, Casal B, Galvan JC. Adv Mater 1995;7:180–4.
[22] Goren M, Qi Z, Lennox RB. Chem Mater 1995;7:171–8.
[23] Zulfiqar S, Shabbir S, Ishaq M, Sarwar MI. J Appl Polym Sci 2009;112:3141–8.
[24] Kim JW, Liu F, Choi HJ, Hong SH, Joo J. Polymer 2003;44:289–93.
[25] Kausar A, Zulfiqar S, Shabbir S, Ishaq M, Sarwar MI. Polym Bull 2007;59:457–68.
[26] Zulfiqar S, Ahmad Z, Ishaq M, Saeed S, Sarwar MI. J Mater Sci 2007;42:93–100.
[27] Kim BH, Jung JH, Hong SH, Joo J, Epstein AJ, Mizoguchi K, et al. Macromolecules 2002;35:1419–23.
[28] Maity A, Ray SS. Macromol Rapid Commun 2008;29:1582–7.
[29] Huang MF, Yu JG, Ma XF. Chin Chem Lett 2005;16:561–4.
[30] Alvi MU, Zulfiqar S, Yavuz CT, Kweon Hee-Seok, Sarwar MI. Ind Eng Chem Res 2013;52:6908–15.
[31] Zulfiqar S, Shah SI, Sarwar MI. Ind Eng Chem Res 2013;52:11050–60.
[32] Park DP, Lim ST, Lim JY, Choi HJ, Choi SB. J Appl Polym Sci 2009;112:1365–71.